Journal of King Saud University – Science 35 (2023) 102689

HOSTED BY

Contents lists available at ScienceDirect

Journal of King Saud University – Science

journal homepage: www.sciencedirect.com

Original article

Development of biomaterial-based oxygen transportation vehicles for circulation within blood

Umit Yasar [a,*], Fatma Ulusal [b], Pınar Yılgor Huri [c], Bilgehan Guzel [d], Nurten Dikmen [e]

[a] Ardahan University, Nihat Delibalta Gole Vocational High School, Ardahan, Turkiye
[b] Mersin Tarsus Organized Industrial Zone Technical Sciences Vocational School, Mersin, Turkiye
[c] Ankara University, Faculty of Engineering, Biomedical Engineering, Ankara, Turkiye
[d] Çukurova University, Faculty of Arts and Sciences, Department of Chemistry, Adana, Turkiye
[e] Çukurova University, Faculty of Medicine, Medical Biochemistry Department, Adana, Turkiye

ARTICLE INFO

Article history:
Received 10 November 2022
Revised 25 March 2023
Accepted 12 April 2023
Available online 20 April 2023

Keywords:
Endothelial cell
Hemoglobin
SPIONs
Artificial blood
Blood substitute

ABSTRACT

Background: Several blood replacements have been developed because of issues with blood collection and storage, increased expenditures, and a global lack of reserves. Studies on artificial blood primarily concentrate on the research and synthesis of molecules that transport oxygen. The primary objective of the current work was to create a supporting, oxygen-carrying biological material that can replace blood and be used to save lives when blood is not available.

Methods: The work started with the synthesis of superparamagnetic iron oxide nanoparticles (SPIONS), and two distinct procedures were applied to ensure binding to hemoglobin (Hb) molecules. The surface modifications of the particles were carried out gradually by 3-amino propyl trimethoxy silane (3APGASPIONS) and tartaric acid (TASPIONS). Analysis methods used to characterize the particles include Fourier transform infrared spectrophotometer (FT-IR), elemental analysis (EDX), scanning electron microscope (SEM), X-ray diffractometry (XRD), and high contrast transmission electron microscopy (C-TEM). The characterization studies of SPIONS which bind Hb molecules to the surface were repeated and their effects on endothelial cell culture were examined to determine their toxic effects in vitro. Cell proliferation, superoxide dismutase (SOD), catalase (CAT), glutathione peroxidase (GPx) activity changes were assessed in the evaluation of the possible toxic effects of the cells against the treated particles in the prepared cell lines. Blood substitute solutions synthesized by two different methods were stored on the shelf for about 1 month and the results were compared with fresh Hb solutions.

Results and Conclusion: The CV and UV analysis results obtained from artificial Hb substitutes revealed that the structural integrity of Hb molecules did not change, the oxygen transport capabilities of biomolecules were preserved, and this state remained stable for a long time. Furthermore, it was determined that nanocomplexes synthesized by the two methods caused different cellular proliferation and there was a more limited increase in cellular enzyme activities (SOD, CAT, GPx) of Hb-bound particle solutions when compared to pure SPIONS.

1. Introduction

The search for a substance that can replace blood, does not require special conditions in the storage, and can be applied to all individuals regardless of the blood group of the recipient has been started a long time ago. The search for an alternative blood substitute to be used in wars and large-scale civil disasters has gradually increased since World war II. It is essential to develop a suitable blood substitute in developing countries due to the reasons such as the decrease in the number of blood donors due to the aging population, the increase in the demand for blood products,

* Corresponding author at: Nihat Delibalta Gole Vocational High School, Ardahan 75100, Turkiye.
E-mail address: umityasar@ardahan.edu.tr (U. Yasar).

Peer review under responsibility of King Saud University.

Production and hosting by Elsevier

https://doi.org/10.1016/j.jksus.2023.102689

the limited storage periods in natural blood products, and the existence of accidents and disasters (Lowe, 1999; Sharma et al., 2011).

However, it is important that the blood to be developed behaves similarly to the natural blood microcirculation in terms of complications associated with blood transfusion. Furthermore, the factors taken into account include not accumulation of the blood substitute in the body, the half-life in the body and the ease of storage conditions (Intaglietta, 1997).

It covers all the substance trials that are considered to replace blood in artificial blood research. The urine, beer, milk, casein derivatives, starch, saline, ringer, perfluorochemicals, hemoglobin-based artificial red blood cells, recombinant hemoglobin (Hb) and red blood cells produced by stem cell differentiation may be included among the substances used in the trials (Keyhanian et al., 2014). Although the development of oxygen therapeutics was a creative idea, many of them failed due to the lack of scientific background (Greenburg and Kim, 2004).

Studies on developing modified Hb have been focused and these studies have increased day by day since it was detected that natural Hb has a toxic effect in human use (Alayash, 2019). Hb solutions prepared by hemolysis of red blood cells were tried in artificial blood transfusion studies performed on rodents, and it was determined that this solution could carry oxygen to the tissues, but had a toxic effect in the liver and caused an increase in the blood pressure (Smith and McCulloh, 2015; Alayash, 2019). In addition, blood transfusion studies with Hb solution showed toxic effects on kidneys and vasoactive formation (Cao et al., 2021a; Ün and Erbaş, 2019). In the light of these developments, pure Hb solutions were focused in the 90s; however, technological developments led up the development of compounds that may carry oxygen to the tissue in the laboratory (Lieberthal et al., 2000). These molecules which cannot be used directly as an oxygen-carrying component have been modified in Hb-based oxygen carriers (HBOC), recombinant Hbs and used as raw materials (Chang, 2004; Kim and Greenburg, 2004; Chang, 2010). Pharmaceutical HBOC was produced as a result of the studies conducted by chemical modification procedures (Lieberthal et al., 2000; Gupta, 2019).

Although they do not completely replace red blood cells perfectly, these "oxygen carrier solutions" have many potential uses, both clinical and non-clinical (Cao et al., 2021b). These substances could reach the tissues more easily than normal red blood cells and transmit oxygen directly to the tissue, and these substances also have side effects (Cao et al., 2021b). Comprehensive clinical trials have been conducted about reliability and benefits of these (Cao et al., 2021b). A better understanding of the modes of action of these products would help to define modes of delivery and benefits (Chang, 1999; Goorha et al., 2003; Takeoka, 2005; Yaşar et al., 2012).

Blood components are mostly interested in the stabilization difficulties of molecules with desired oxygen carrying capacity and affinity (TJ, 2003; Greenburg and Kim, 2004). Although extensive knowledge has been gained about the functions and oxygen carrying capacities of these components, the searches and seeking for alternative artificial blood continues (Chang, 2006; Sarkar, 2008; Chang, 2010).

SPIONs are commonly used in recent clinical development studies (Kim et al., 2006). The purposes of use include nucleic acid, peptide and drug carrying (Arami et al., 2015). Particle surface properties should be prepared in detail and made suitable for study (such as adsorption, size, distribution) in this type of development studies (Arami et al., 2015). Such particles focused on clinical trials have been approved for anemia treatment (US food and drug administration-FDA-) (Abo-Zeid et al., 2020). Tissue distribution of these molecules during and after clinical diagnosis and therapeutic procedures is accepted as a biological distribution (Arami et al., 2015).

We present a solution that may be developed as an alternative to the aforesaid artificial blood substitutes and in therapeutic use with a longer shelf life, lower antigen activity, stabilization of Hb molecules with the correct surface modifications of SPIONs. Two different methods were used in this study. First method was blood substitutes developed as TASPIONS and the second method was 3APGASPIONS.

2. Materials and methods

2.1. Chemicals, equipment, and analyses

Ethanol (C_2H_5OH), sodium hydroxide (NaOH), sodium chloride (NaCl), tartaric acid ($C_4H_6O_6$), iron (II) sulfate monohydrate ($FeSO_4 \cdot H_2O$), iron(III) chloride hexa chloride ($FeCl_3 \cdot 6H_2O$), 3-(aminopropyl) trimethoxy silane ($H_2N(CH_2)_3Si(OCH_3)_3$), glutaraldehyde ($C_5H_8O_2$), sodium boron hydride ($NaBH_4$), pyridinium chloro chromate (PCC), HEPES Buffer, human Hb (Sigma Aldrich) were obtained in the cell culture. Dulbecco's modification of Eagle's medium (DMEM), fetal bovine serum (FBS) and Hank's balanced salt solution (HBSS) were obtained from Biochrome. The HEPES, penicillin streptomycin santibiotics (PSA), Trypsin/EDTA, methylthiazole diphenyl tetrazolium (MTT), phosphate buffer (PBS), fetal bovine serum (FBS) and dimethyl Sulfoxide (DMSO) were obtained from Sigma Aldrich. The human umbilical vascular endothelial cell (HUVEC) line obtained from the Department of Biology, Faculty of Arts and Sciences, Middle East Technical University (METU), Turkey was used in the experiments. The kits used in the study were methylthiazole diphenyl tetrazolium (MTT) -(3-[4 ,5-dimethylthiazole-2-yl]-2,5-diphenyltetrazolium bromide, thiazolyl blue), catalase (CAT) measurement kit, superoxide dismutase measurement kit (Biovision) and glutathione peroxidase measurement kit (Randox). Elemental analysis (Thermo Scientific Flash 2000, CHNS), FT-IR spectroscopy (Thermo FT-IR spectrophotometer; Smart ITR diamond attenuated total reflection (ATR); 4000–400 cm^{-1}), scanning electron microscope (SEM); Jeol JSM-5500 LV, transmission electron microscopy (cTEM); FEI Tecnai G2 Spirit BioTwin C-TEM, X-ray diffractometer (XRD), Rigaku miniflex CuKα, λ = 0.154 nm, UV–vis spectrometer; Perkin elmer lambda 25, magnetic stirrer heater; Velp, WiseStir, cyclic voltogram; CHI 604, Serial No: 64721A, ultrasonic homogenizer; bandelin sonopuls, biosafety cabinet class II; berner B-(MaxPro)2-130, CO_2 incubator and heal force. Other materials and chemicals were present in the laboratories of Cukurova University, Adana, Turkey. The CV analysis was performed in the suspension prepared as 3 mg TASPIONs-Hb/10 mL and 3 mg 3APGASPIONs-Hb/10 mL phosphate solution in pH 7.4 phosphate buffer, at a scanning rate of 100 mV. s^{-1} carried out in the same solution as 3 cycles of repetitions. The C-Tem analyses were performed in METU, elemental analyses were conducted in Mersin University, Meitam/Mersin, and the cell culture and UV–vis analyses were carried out in Medical Biochemistry Department, Cukurova University, Faculty of Medicine.

2.2. The synthesis of the superparamagnetic iron oxide nanoparticle support material (SPIONs)

Iron (II, III) oxide SPIONs were obtained according to the method used by Mahmood et al. (2013). A 2.3377 g (8.6 mmol) of $FeCl_3 \cdot 6H_2O$ and 0.7347 g (4.33 mmol) of $FeSO_4 \cdot H_2O$ were dissolved in 100 mL of distilled water and heated to 90 °C with vigorous stirring in a nitrogen atmosphere with a mechanical stirrer. Initially, 12 mL of 0.1 M NaOH solution was slowly added to this mixture and mixed. The mixture of iron salts was yellow at the beginning, black nanoparticles appeared on places where NaOH drops have fallen. Then, 12 mL of 0.3 M NaOH solution was added

to allow termination of the precipitation. Such mixture was separated through magnetic decantation after completion of precipitation. It was irrigated with pure water. The SPIONs obtained were dried in a vacuum desiccator (Mahmood et al., 2013).

2.2.1. Coating of the particle

2.2.1.1. Coating of SPIONS by tartaric acid. Coating of SPIONs with tartaric acid was performed through the method used by Mahmood et al. (2013). One g of SPIONs was suspended in 100 mL of distilled water by ultrasonic bath for 30 min in coating. 0.5 g of tartaric acid was added to this mixture and mixed vigorously with a mechanical mixer for 1 h at room temperature. Then, the mixture was mixed in the ultrasonic bath for 1 h and separated by decantation. Finally, it was washed with distilled water until no free tartaric acid remained. The SPIONs coated by tartaric acid (TASPIONs) was dried in vacuum desiccator. One g of TASPIONs was suspended in 100 mL distilled water by ultrasonic bath in surface modifications for TASPIONs to be used in Hb immobilization. 0.1 g of $NaBH_4$ was added to this mixture and it was mixed vigorously with a mechanical mixer for 2 h. The alcohol coated SPIONs obtained were separated through magnetic decantation. They were dried in vacuum desiccator (Simek et al., 1997). Approximately 1 g was taken then and suspended in 100 mL of acetone with an ultrasonic bath for the chemical ends to gain an aldehyde structure. 0.1 g PCC was added and it was mixed at room temperature for 24 h and the alcohol groups were converted to aldehyde within this period (Al-Hamdany and Jihad, 2012). The obtained aldehyde coated SPIONs were magnetically separated, washed with acetone until no PCC residue remained, and dried in a vacuum desiccator.

2.2.1.2. Coating of SPIONs with 3-(aminopropyl) trimethoxysilane and surface modification with glutaraldehyde. Two g of SPIONs was suspended in 100 mL of acetone by ultrasonic bath for 30 min. After 10 min of sonication, 4 mL of 4 % 3-(aminopropyl) trimethoxy silane solution prepared in distilled water was added. This mixture was magnetically stirred at 45 °C for 24 h. The 3-(aminopropyl) trimethoxysilane coated SPIONs obtained at the end of this period were washed with distilled water until there was no residue and dried in an oven at 115 °C overnight. For transformation of amine groups to aldehydes, 25 mL of phosphate buffer (pH 7.4) was added onto 1.97 g coated SPIONs and suspended in an ultrasonic bath. Twenty-five g (62.7 mmol) of 25 % glutaraldehyde solution was mixed vigorously with a mechanical mixer at room temperature for 3 h. At the end of this period, it was washed with distilled water until there was no free glutaraldehyde through magnetic decantation. It was dried in an oven at 50 °C (Tang et al., 2011).

2.3. Hb immobilization to SPIONs

The target at this stage was to stabilize and immobilize the modified SPIONs, which were coated with the previously mentioned chemicals through various steps, by forming Schiff base compounds with Hb molecules by using different arms. One mg of modified aldehyde-coated SPIONs suspended in an ultrasonic homogenizer in 3 mL pH 7.4 phosphate buffer under nitrogen (N_2) gas circulation were used for immobilization of Hb on modified SPIONs. Ten ml of phosphate buffer at pH 7.4 dissolved in 7 mg of pure Hb (Hb was purified at some stages (Mohanto et al., 2022) was added. The mixture with an Hb molarity of 8.35x10-9 M was mixed at room temperature with a rotator at 100 rpm for 5 h, after which it was exposed to a magnetic field to separate all SPIONs-Hb. This procedure was repeated by washing with phosphate buffer at pH 7.4 for 5 times. The SPIONs-Hb obtained were stored in the flow cabinet in phosphate buffer at pH 7.4 to be used when needed (approximately 1 month).

2.4. Assessment of cytotoxicity and cell proliferation

The HUVEC line was used in our study. The cells were incubated in an incubator at 95 % humidity and 5 % CO2 at 3 °C. The cell culture work-ups were performed in a laminary class type II cabinet sterilized by ultraviolet. After trypsinization of the cells in the 75 cm^2 flask, the cells obtained were counted manually (Fig. 1). A cell suspension of 30 µl and 100 µl of cell medium were added to each well to be homogeneous and homogenized on a 96-well flat plate. The culture plate was then placed in the incubator and the cells were allowed to adhere to the plate surface for 24 h. The plate was taken away on the next day, and the effect on endothelial cell proliferation and vitality was investigated. Ten (10) µl of homogeneous blood substitute (Fig. 1) was added to each well and MTT analysis was performed in the determination of endothelial cell proliferation and cytotoxicity. The color change detected was measured through a spectrophotometer at absorbency of 570 nm.

2.5. The examination of the effects of SPIONs complexes on antioxidant enzyme activities

Thirty (30) µl of cell suspension was added equally and homogeneously to each well of 4 culture plates with 24 wells, and 1 mL of cell medium was placed on each well, allowing the cells to be homogeneously dispersed in the well. The culture plates were placed in the incubator and the cells were allowed to adhere to the plate surface for 24 h. After the medium on the cells was removed after incubation, 10 µl (1 mg/10 mL PBS), pure SPIONs, pure Hb, 3APGASPIONs-Hb and TASPIONs-Hb solutions and 1 mL cell medium were added to each well. A control group was created by adding 1 mL of cell only medium to 12 wells. Each experimental set was analyzed on eight experimental groups like in the proliferation analysis. Culture plates were placed in the incubator for 72 h of incubation of cells with solutions. The cell medium in the plate was carefully removed and the cells were washed twice with PBS at the end of the incubation period. After the PBS was removed, 1 mL of lysis buffer was added to each well and incubated at 37 °C for 5 min. The solution containing the cell fragments in each well was withdrawn after observing the disintegration of the cells under an inverted microscope and taken into 2 mL sterile Eppendorf tubes and centrifuged at 10,000 g for 15 min. After centrifugation, the supernatant parts were taken into sterile Eppendorf tubes; samples were created and placed into a freezer at −20 °C for antioxidant studies.

3. Results

3.1. The synthesis of the support material (SPIONs)

Two characteristic peaks of 3000–3450 cm^{-1} and 584 cm^{-1} were observed when the FT-IR spectrum of the synthesized SPIONs was examined. Characteristic peaks 220, 311, 400, 422, 511 and 440 belonging to Fe_3O_4 were observed when XRD spectrum was examined. The particle size was calculated by Debye-Scherrer equation. The data of peak 311 which is the basic peak was used for the size. Accordingly, the particle size was calculated as 20 nm. Their sizes were in the range between 10 and 50 nm when the C-TEM images of SPIONs are examined. From the C-TEM images, the size of each particle cluster was determined to be in the range between 100 and 250 nm.

3.2. SPIONS coating by tartaric acid

Characteristics peaks were observed at 3000–3300 cm^{-1}, 1595 cm^{-1}, 1084 cm^{-1} and 602 cm^{-1} when FT-IR spectrum was

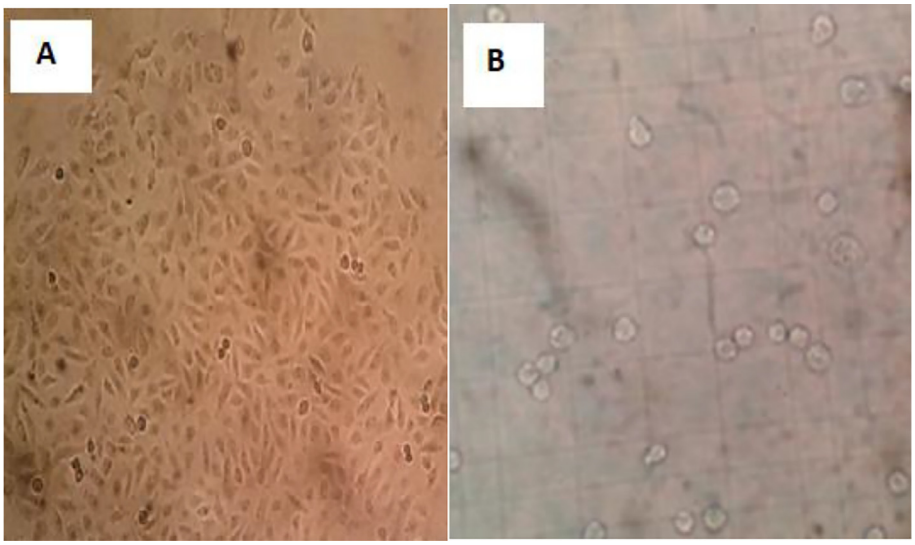

Fig. 1. Endothelial cell culture inverted microscope image (X40) (A) and endothelial cells in thoma slides examination (B).

reviewed after tartaric acid coating of the support. Characteristic peaks 220, 311, 400, 422, 511 and 440 belonging to Fe_3O_4 were observed when XRD spectrum was examined. The particle size was calculated by Debye-Scherrer equation. Accordingly, the particle size was calculated as 21.1 nm. It was detected that the sizes were smaller than 50 nm in line with Sem and C-TEM data. The amount of coating was found as a percentage from the EDX data obtained after coating, according to which 1.7x10-3 mol tartaric acid/g SPIONs coating was realized.

3.2.1. Reduction of carboxylic acid group, oxidation of alcohol groups

$NaBH_4$ is a strong reducing agent, reducing carboxylic acids up to the alcohol level. Review of the FT-IR results revealed peaks at 3000–3650 cm^{-1}, 1646 cm^{-1}, 1409 cm^{-1}, 1083 cm^{-1} and 588 cm^{-1}. The size of XRD spectrum was calculated as 21.1 nm. Characteristics peaks were observed at 3000–3650 cm^{-1}, 1403 cm^{-1}, 587 cm^{-1} and 587 cm^{-1} when FT-IR spectrum of aldehyde-coated SPIONs was reviewed after PCC stage. C-TEM images showed that the particles were also approximately below 50 nm in size. SEM and XRD analyzes and EDX results showed that the coating has taken place.

3.3. Coating and modification of SPIONs with 3-(Aminopropyl) trimethoxysilane

Peaks were observed at −1634 cm^{-1}, 1049 cm^{-1}, 2975 cm^{-1}, 1110 cm^{-1} and 586 cm^{-1} when the FT-IR spectrum of 3-(Aminopropyl) trimethoxysilane coated SPIONs is examined. The mean size in XRD spectrum results is 22.8 nm. When the C-TEM images are examined, it could be said that the particle size varies in the range below 50 nm, and the SEM results are similar. Peaks were observed at 3001 cm^{-1}, 1665 cm^{-1}, 1553 cm^{-1}, 1091 cm^{-1}, 593 cm^{-1} when the FT-IR spectrum of glutaraldehyde surface modification. The particle size of XRD spectrum was calculated as 23.3 nm. The size below 50 in SEM and C-TEM images and increase of carbon atom is observed in EDX results.

3.4. Hb binding to modified SPIONs

TASPIONS-HB, when FT-IR spectrum was reviewed, peaks at 3000–3600 cm^{-1}, 3050–3100 cm^{-1}, 2922 cm^{-1}, 1644 cm^{-1}, 1531 cm^{-1} and 584 cm^{-1} (Fig. 2). Particle sizes were calculated from the Debye-Scherrer equation, and the particle size was calculated as 24.2 nm accordingly (Table 1). When the UV–vis spectrum of fresh pure Hb was examined, it gave two characteristic peaks at 539.72 and 577.18 nm (Fig. 3). Characteristic peaks were observed in TASPIONs and pure Hb UV–vis measurements made after waiting for about 1 month from the treatment steps (Fig. 3). When C-TEM images of TASPIONs-Hb were examined, they showed that they were approximately 50–200 nm in size. This is also true for SEM analysis (Fig. 4). The carbon atom increase in the EDX analysis results was also determined (Fig. 2).

Hb has received oxygen and peaked at −0.418 V cathodic potential against Ag/AgCl standard electrode. The Hb gave the oxygens taken and provided a peak at −0.145 V anodic potential. When the CV of the solution containing only Hb was examined, a peak at −0.468 V cathodic potential and −0.06 V anodic potential was observed against Ag/AgCl standard electrode (Fig. 5).

3APGASPIONs-HB, when FT-IR spectrum was reviewed, peaks at 3000–3600 cm^{-1}, 3054 cm^{-1}, 2913 cm^{-1}, 1639 cm^{-1}, 1531 cm^{-1} and 587 cm^{-1} (Fig. 6). Particle sizes were calculated from the Debye-Scherrer equation, and the particle size was calculated as 25.3 nm accordingly (Table 2). When the UV–vis spectrum of fresh pure Hb was examined, it gave two characteristic peaks at 539.72 and 577.18 nm (Fig. 3). Characteristic peaks were observed in 3APGASPIONs measurements made after waiting for about 1 month from the treatment steps (Fig. 3). When C-TEM images of 3APGASPIONs-Hb were examined, they showed that they were approximately below 50 nm in size. This is also true for SEM analysis (Fig. 7). The carbon atom increase in the EDX analysis results was also determined (Fig. 6).

The Hb molecule provided an oxidation peak at the cathodic potential of −0.398 V against the Ag/AgCl standard electrode. The Hb gave the oxygens taken and provided a peak at −0.136 V anodic potential. When the CV of the solution containing pure Hb was examined, a peak at −0.468 V cathodic potential and −0.06 V anodic potential was observed against Ag/AgCl standard electrode (Fig. 5).

3.5. The effect of synthesized complexes on endothelial cell viability and proliferation

In our study, it was determined that pure SPIONs, pure Hb and 3APGASPIONs-Hb complexes applied on endothelial cells increased cell viability and proliferation ($p < 0.01$); application of TASPIONs-

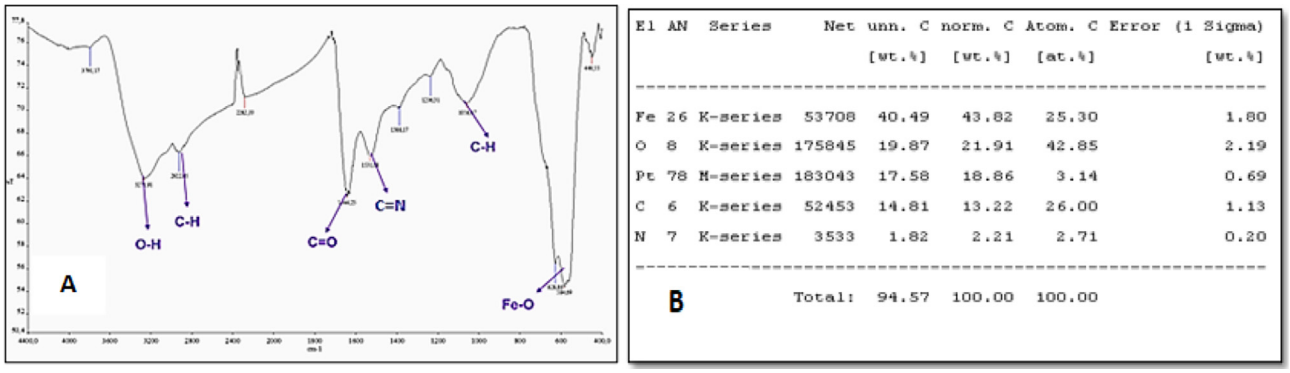

El	AN	Series	Net unn. C [wt.%]	norm. C [wt.%]	Atom. C [at.%]	Error (1 Sigma) [wt.%]
Fe	26	K-series	53708	40.49	43.82	25.30	1.80
O	8	K-series	175845	19.87	21.91	42.85	2.19
Pt	78	M-series	183043	17.58	18.86	3.14	0.69
C	6	K-series	52453	14.81	13.22	26.00	1.13
N	7	K-series	3533	1.82	2.21	2.71	0.20
		Total:		94.57	100.00	100.00	

Fig. 2. The FT-IR spectrum of Hbs bound to tartaric acid coated SPIONs (A) and TASPIONs-Hb EDX elemental analysis results (B).

Table 1
The XRD analysis of Hbs bound to tartaric acid-coated SPIONs.

No.	2-theta (deg)	D (ang.)	Height (cps)	FWHM (deg)	Int. I (cps deg)	Int. W (deg)	Size (A)
1	30.103(15)	2.9662(14)	179(12)	0.379(13)	91.6(18)	0.51(5)	227
2	31.619(11)	2.8274(9)	92(9)	0.163(14)	19.9(13)	0.22(3)	120
3	35.362(11)	2.5362(7)	390(18)	0.30(6)	175(58)	0.45(17)	232
4	35.494(15)	2.5270(10)	337(17)	0.28(3)	138(58)	0.41(19)	233
5	43.140(16)	2.0952(7)	133(11)	0.376(13)	64.3(13)	0.48(5)	256
6	45.331(9)	1.9989(4)	59(7)	0.13(2)	12.7(7)	0.22(4)	23.1
7	53.63(3)	1.7074(7)	56(7)	0.43(4)	31.6(13)	0.56(9)	190
8	57.087(19)	1.6121(5)	164(12)	0.440(17)	95.5(17)	0.58(5)	225
9	62.727(16)	1.4800(3)	242(14)	0.423(13)	132.3(19)	0.55(4)	235

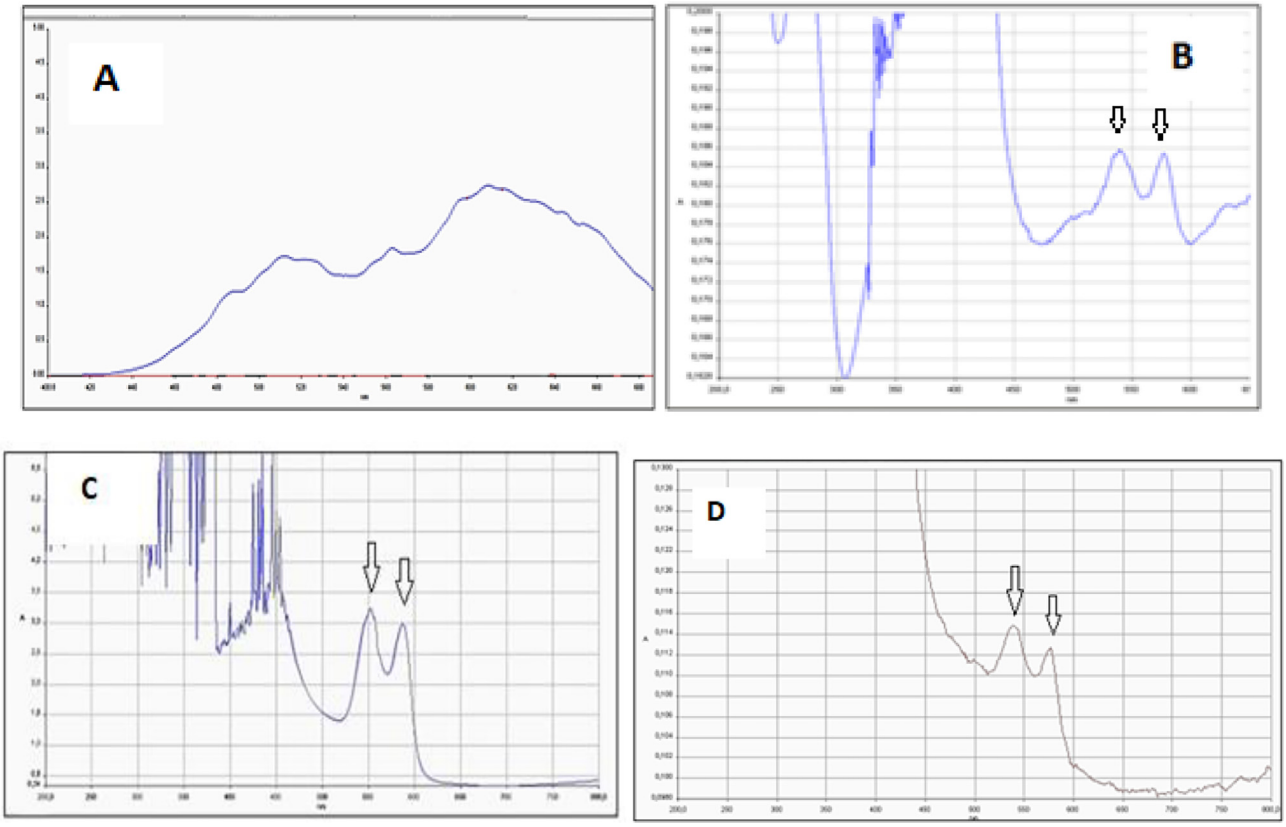

Fig. 3. Stored at room temperature for approximately 1 h, free Hb UV–vis spectrum (A), TASPIONs UV–vis spectrum (B) UV–vis spectrum of oxyhemoglobin (C), and 3APGASPIONs UV–vis spectrum (D).

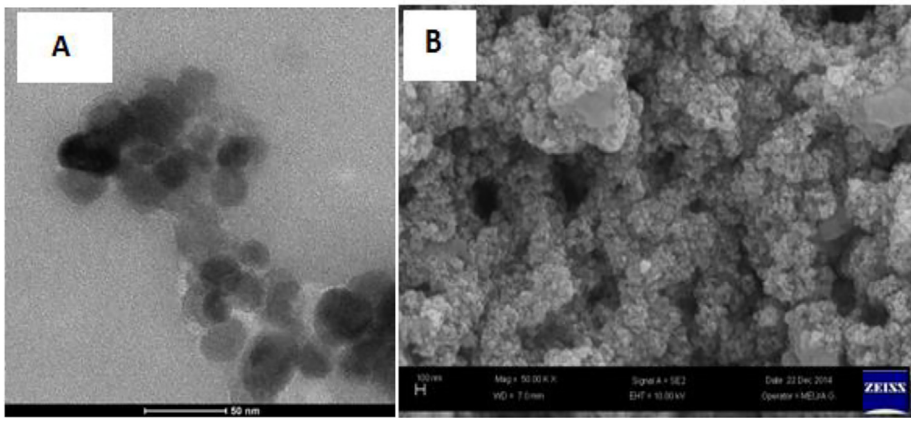

Fig. 4. The TASPIONs-HB C-TEM image (A), and TASPIONs-Hb SEM image (B).

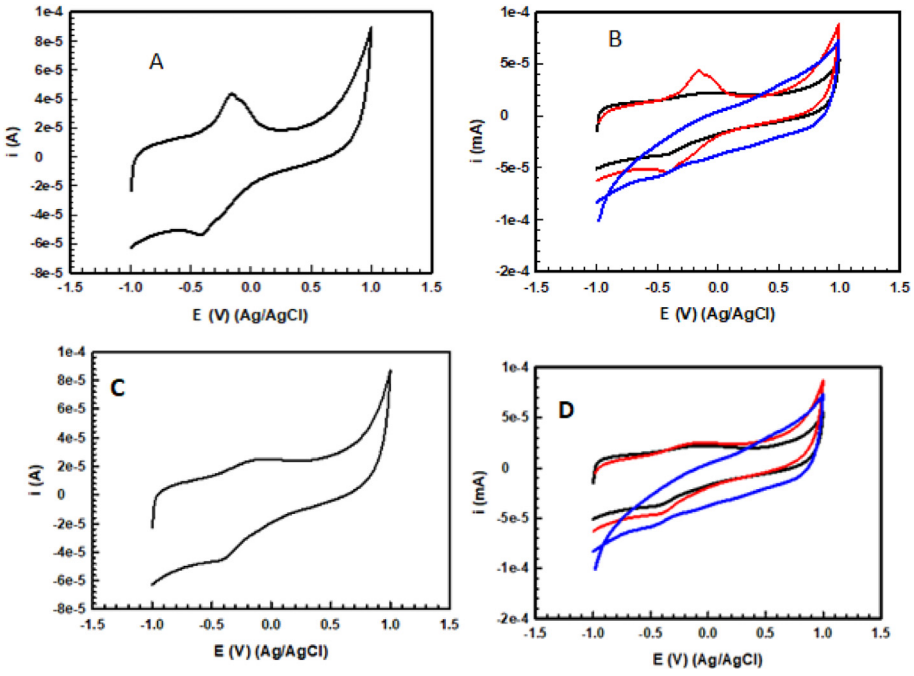

Fig. 5. CV TASPIONs-Hb (A) CV (pure Hb, TASPIONs-Hb, TASPIONs) (B) CV 3APGASPIONs-Hb (C) CV (pure Hb, 3APGASPIONs-Hb, 3APGASPIONs) (D).

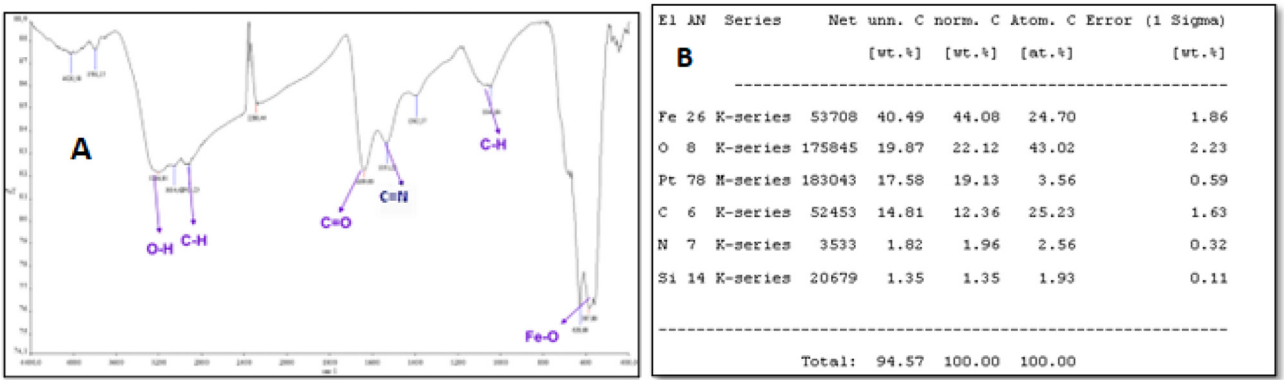

B

El	AN	Series	Net unn. C [wt.%]	norm. C [wt.%]	Atom. C [at.%]	Error (1 Sigma) [wt.%]
Fe	26	K-series	53708	40.49	44.08	24.70	1.86
O	8	K-series	175845	19.87	22.12	43.02	2.23
Pt	78	M-series	183043	17.58	19.13	3.56	0.59
C	6	K-series	52453	14.81	12.36	25.23	1.63
N	7	K-series	3533	1.82	1.96	2.56	0.32
Si	14	K-series	20679	1.35	1.35	1.93	0.11
		Total:		94.57	100.00	100.00	

Fig. 6. 3APGASPIONs-Hb FT-IR spectrum (A) 3APGASPIONs-Hb EDX elementary analysis results (B).

Table 2
3APGASPIONs-Hb XRD data.

No.	2-theta (deg)	D (ang.)	Height (cps)	FWHM (deg)	Int. I (cps deg)	Int. W (deg)	Size (A)
1	30.11(19)	2.96(19)	177(17)	0.37(18)	94(2)	0.53(6)	223
2	31.60(8)	2.82(7)	34(7)	0.26(6)	11.9(18)	0.35(13)	126
3	35.45(12)	2.52(9)	574(31)	0.37(10)	288(4)	0.50(3)	253
4	43.17(2)	2.09(11)	114(14)	0.40(19)	53(2)	0.47(7)	235
5	53.63(5)	1.70(16)	56(10)	0.49(5)	34.2(19)	0.61(14)	156
6	57.10(3)	1.61(7)	172(17)	0.42(2)	102(2)	0.59(7)	132
7	62.73(2)	1.47(5)	256(21)	0.38(19)	138(3)	0.54(5)	138

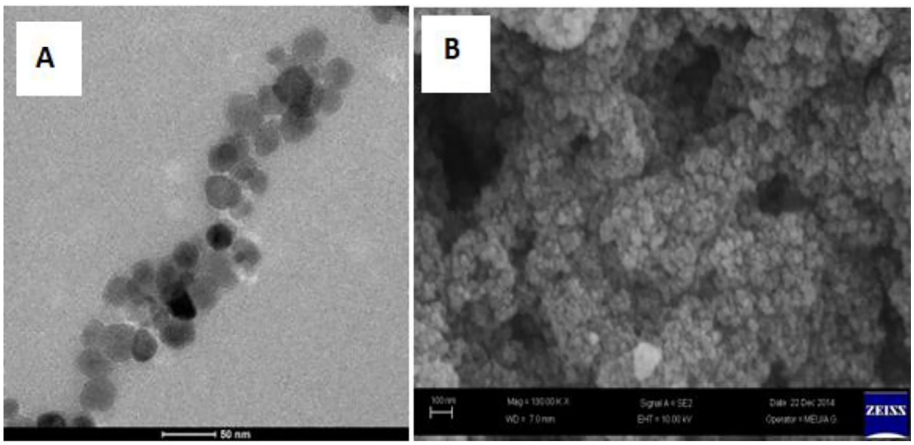

Fig. 7. 3APGASPIONs-HB C-TEM image (A) 3APGASPIONs-Hb SEM image (B).

Hb complex did not cause a statistically significant increase in proliferation and cell viability. (Table 3).

3.6. The effects on antioxidant enzyme defense

It was determined that CAT ($p < 0.01$), SOD($p < 0.05$) and glutathione peroxidase ($p < 0.01$) enzyme activity increased significantly in pure SPIONs application when compared to control. Pure Hb administration to endothelial cells did not cause a statistically significant change in the CAT enzyme activity. It was determined that it caused a significant increase in SOD ($p < 0.001$) and glutathione peroxidase ($p < 0.01$) activities. While 3APGASPIONs-Hb administration did not cause a significant change in the CAT and SOD enzyme activity of the endothelial cell; it was determined that it decreased the GPX activity. In our study, the application of TASPIONs-Hb complex on endothelial cells did not cause a statistically significant change in CAT and SOD enzyme activity; however, it significantly increased GPX activity ($p < 0.01$).

4. Discussion

4.1. SPIONs synthesis

The review of FT-IR spectrum of pure SPIONs revealed that the O-H vibration was determined at 3000–3450 cm^{-1}. Although the chemical formula of SPIONs is Fe_3O_4, Tang et al. reported that the surface of SPIONs is covered with an OH layer. This O-H peak is caused by the OH layer on the surface of SPIONs (Mahmood et al., 2013). A characteristics Fe-O tension peaj was observed at 584 cm^{-1} (Tang et al., 2011). The main peak of Fe_3O_4 was found 311 with XRD results and spinel particle sizes were calculated below 50 nm by the Debye-Scherrer equation (Tang et al., 2011; Mahmood et al., 2013). C-TEM results are like XRD. Results obtained showed that particles below 50 nm. However, as stated in the literature, agglomeration is observed. In our study, agglomeration cluster sizes are in the range of about 100–250 nm (Rezaeifard et al., 2012; Liu et al., 2014). It was stated in the literature that particles below 50 nm is super paramagnetic. The C-TEM and XRD results of this study showed that the synthesized spherical particles were superparamagnetic (Lu et al., 2002).

4.1.1. SPIONS coating by tartaric acid and modification

The expected peaks in the FT-IR spectrum were observed in the characterization of the tartaric acid coated particle. These peaks are C=O double bond originating from tartaric acid, aliphatic C-H vibration peaks and O-H stretching peaks. The review of FT-IR spectrum of pure revealed that the O-H vibration peaks were determined at 3000–3300 cm^{-1}. Although this peak is the O-H peak in the carboxylic acid group of tartaric acid, it is also due to the OH layer around Fe_3O_4 (Mahmood et al., 2013). Although this

Table 3
The absorbance values (OD) obtained in the cell proliferation study of the experimental groups.

Samples	N	Minimum	Maximum	Mean	Standard Deviation
Control	8	0.56	0.76	0.63	0.07
Pure SPIONs	8	0.58	1.14	0.86	0.18
Pure Hb	8	0.63	0.95	0.77	0.12
3APGASPIONs-Hb	8	0.62	0.84	0.76	0.07
TASPIONs-Hb	8	0.45	1.27	0.75	0.27

peak is the O-H peak in the carboxylic acid group of tartaric acid, it is also due to the OH layer around Fe_3O_4. It was observed at 1595 cm^{-1} in the functional group region. The presence of both OH and C=O peaks indicates the carboxylic acid in the structure. Another peak originating from tartaric acid is aliphatic C-H vibration peaks. Unlike SPIONs, a C-H stretch peak was observed at 1084 cm^{-1}. The Fe-O tension peak was observed at 602 cm^{-1}, similar to SPIONs (Tang et al., 2011; Mahmood et al., 2013; Liu et al., 2014). This was seen at a higher wave frequency when encountering SPIONs. The reason for this effect is the electrophilicity of the carboxylate group in the Fe-O-C(=O)-R structure formed by the bonding, namely, electron attractiveness of tartaric acid. The electrophilic property may cause a decrease in electron density in oxygen, which may result in a shortening of the Fe-O bond. The shortening of the bond causes an increase of the energy required to stimulate the bond. The increase in energy decreases the wavelength, which is inversely proportional to the frequency, so the frequency increases (Darendeli, 2014).

Our XRD results showed characteristic peaks; however, a slight rightward shift was observed. The shift has two reasons. The first of these is the decrease in the residual stress between the solid materials, the other is the change of the positions of the atoms in the crystal lattice with respect to each other and the change of parameters such as the bond lengths and angles of the atoms in the standard crystal. The shifts in the fundamental peaks after coating in SPIONs are due to the changes in the positions of the atoms in the crystal lattice (Özdemir, 2006). Based on this information, it could be said that the crystal lattice of SPIONs among SPIONs remains intact during the surface coating process. Particle sizes were calculated as 21.1 nm using the 311 peak from the Debye-Scherrer equation (Yaşar, 2016). When the C-TEM, SEM and XRD results are evaluated together, the size and coating properties support each other. The particle sizes are below 50 nm, they are small, and the coating occurred. The amount of coating was found as a percentage from the EDX data obtained after coating, according to which 1.7x10-3 mol of tartaric acid/g SPIONs coating has occurred. O-H vibration peaks of alcohol groups with surface modification with NaBH4 were observed at 3000–3650 cm^{-1} as expected. The O-H bond was also found at 1409 cm^{-1} on the fingerprint region. The Fe-O peak was observed at 588 cm^{-1}. The C=O tension peak was observed at 1646 cm^{-1} as in tartaric - coated particles (Tang et al., 2011; Jadhav et al., 2013; Mahmood et al., 2013). Weaker and higher waves than the tartaric acid-coated particles are the reduction of the carboxylic acid itself to alcohol, which has less electrophilic properties. This means that the energy required to stimulate the bond is reduced due to the extension of the bond. The decrease in energy also increases the wavelength and decreases the number of waves (Shriver et al., 1999).

When the XRD spectrum of alcohol-coated SPIONs was examined, it was shown that the crystal lattice of SPIONs remained in the spinning structure. (Mahmood et al., 2013). It can be said that the crystal lattice of SPIONs remains intact during the surface coating and modification processes (Yaşar, 2016). The particle size is 21.3 nm. The review of all data clearly reveals that the tartaric acid group of the tartaric acid- coated SPIONs is reduced to alcohol. There are three alcohol groups including one primary and two secondaries in the particles after the NaBH4 step. The treatment with PCC caused the conversion of primary alcohol group to aldehyde, and the secondary alcohol groups to ketones. When the FT-IR spectrum of the obtained aldehyde and ketone coated SPIONs was reviewed, it was observed that the O-H vibration peaks of the alcohol groups were similar to the others at 3000–3650 cm^{-1}, as expected. The O-H bond was also found at 1403 cm^{-1} on the fingerprint region. The Fe-O peak was observed at 587 cm^{-1}. The reason for the decrease in the wave number (frequency) is the functional group changes. As the electrophilic property increases, the electron density on the oxygen atom in the Fe-O-C(=O)-R structure decreases. This causes shortening of the Fe-O bond. The shortening of the bond causes an increase in energy and a decrease in the number of waves (Shriver et al., 1999). The Fe-O peak was observed at 588 cm^{-1} in alcohol-coated form; however, it was observed at 587 cm^{-1} in aldehyde structure. The C=O peak was observed at 1627 cm^{-1} as expected. According to C-TEM, SEM and EDX results, it is possible to say that the dimensions are <50 nm and that the coating and its modification have taken place.

4.1.2. Coating of SPIONs with 3-(Aminopropyl) trimethoxysilane, modification

Coating with 3-(Aminopropyl) trimethoxysilane seems to overcome the agglomeration problem of SPIONs [29]. Some characteristic peaks are expected to be observed from the FT-IR spectrum of the coated particles. These peaks are mainly the vibration peaks of the Fe-O-Si bond and the C-H vibration peak which is formed by binding of 3-(Aminopropyl) trimethoxysilane to SPIONs. The Fe-O-Si vibration peak was observed at 1634 cm^{-1} when the FT-IR spectrum was examined. In the fingerprint region, the Fe-O-Si peak was observed at 1049 cm^{-1} (Tang et al., 2011). These peaks indicate that 3-(Aminopropyl) trimethoxysilane is attached to SPIONs by chemical bonding. However, the point to be noted here is that during the bonding of 3-(Aminopropyl) trimethoxysilane, the methoxy groups are separated by hydrolysis and bonded to SPIONs via the silicon atom. Another peak obtained in the spectrum of 3-(Aminopropyl) trimethoxysilane coated SPIONs is the aliphatic C-H vibration peaks. This peak was detected as a vibration peak at 2975 cm^{-1} and a stretching peak at 1110 cm^{-1} of SPIONs. The Fe-O peak was observed at 590 cm^{-1} in SPIONs; however, it was observed at 586 cm^{-1} in 3APSPIONs. This peak was detected at a lower wavenumber when compared to SPIONs. The reason for the peak shift is that the bonded group in the Fe-O-Si-R structure is the electron donor group. The Fe-O bond thereby prolongs, and the energy required to stimulate the bond decreases along with the prolongation. XRD, SEM and C-TEM images of particles coated with 3-(Aminopropyl) trimethoxysilane support each other (<50 nm). The analysis shows that the coating takes place and that the coating does not occur at the same level for each particle. Furthermore, C-TEM images show that the agglomeration caused by pushing to the weak molecule given by the existing coating is reduced. It has been concluded that the slight right shift of the XRD fundamental peaks of the particles in which the spinel and spherical structure is preserved is due to the changes in the positions, angles and interactions of the atoms in the crystal lattice. The expected peaks of FT-IR analysis after glutaraldehyde coating are Fe-O-Si, C=N from Schiff Base and C=O, C-H vibration peaks from aldehyde in glutaraldehyde. The Fe-O-Si and C=O vibration peaks were observed at 1665 cm^{-1} in our results. The peak observed at 1091 cm^{-1} on the fingerprint region is an indication of the presence of C-O. (Mahmood et al., 2013). This peak also belongs to the Fe-O-Si peak. This peak was created by the overlapping of the Fe-O-Si and C-O peaks. The fact that the Fe-O-Si peak is more intense than before the coating shows the success of the coating. As expected, the aliphatic C-H peak was found at 3001 cm^{-1}, the Fe-O stress peak was at 593 cm^{-1}, and the C=N vibration peak of the Schiff base was found at 1553 cm^{-1} in line with the literature (Chawla and Pundir, 2011; Tang et al., 2011; Mahmood et al., 2013; Liu et al., 2014). XRD, C-TEM and SEM results support each other (<50 nm). Aggregation was in the range between 50 and 200 nm, and the increase of carbon atom according to EDX results showed glutaraldehyde binding (Özdemir, 2006; Chawla and Pundir, 2011; Tang et al., 2011; Mahmood et al., 2013).

4.1.3. Hb modification of TASPIONs and 3APGASPIONs

The amine (-NH_2) groups in the asparagine, glutamine, lysine, and arginine amino acids in the Hb molecule bind to the aldehyde groups of SPIONs synthesized by two different methods, forming a Schiff base (C=N). When the TASPIONs-Hb obtained and 3APGASPIONs-Hb FT-IR spectra were examined, it was seen that they were similar to the FT-IR spectrum obtained from pure Hbs encountered in the literature (Polakovs et al., 2012). In both methods, it shows the presence of O-H groups with broad and intense peak structure observed at 3000–3600 cm^{-1}. These OH peaks are thought to originate from the amino acid in the Hb molecule and the carboxylic acid groups in the heme group(Arnone, 1974). The peak observed at 3054 cm^{-1} at 3050–3100 cm^{-1} in TASPIONs and 3APGASPIONs, respectively, is the C-H vibrational peak of the aromatic ring originating from phenylalanine, tryptophan, trosine and histidine. Peaks due to Fe-O vibration were observed at 584 cm^{-1} and 587 cm^{-1}. Aliphatic C-H vibration peaks from Hb and support material as expected. At 2922 cm^{-1} and 2913 cm^{-1}, similar to the literature, the C=O group which is one of the basic groups from the structure of amino acids that make up Hb, was observed at 1644 cm^{-1} and 1639 cm^{-1}. The presence of both OH and C=O bonds indicates the presence of Hb due to the carboxylic acid in the structure [36]. Hb binds to TASPIONs and 3APGASPIONs by forming a Schiff base (C=N). There is a C=N bond in the heme group of Hb. The C=N bond from these two sources was observed as a strong peak at 1531 cm^{-1}. Based on these data, it could be said that the Hb molecule binds successfully in both methods.

When the UV–vis spectra were examined after about 1 month on the shelf, peaks were observed at 539.72 and 577.18 nm and 539.72 and 577.18 nm in TASPIONS and 3APGASPIONS, respectively. These peaks overlap with two characteristic peaks of oxyhemoglobin at 540.37 and 578.47 nm. In this case, it can be said that Hb do not lose their function after binding and are in the form of oxyhemoglobin (Herold, 1998). However, this is not the case with held unbound Hb. The analyzes showed that unbound Hb molecules gave a spectrum similar to the methemoglobin spectrum. It may be stated that Hb binding to SPIONs increases stability. In both techniques, XRD, C-TEM and SEM images showed size (<50 nm) and Hb binding, but the difference in the organic layer suggested that the number of bound Hb per particle might also be different. When the EDX data are compared, it can be concluded that the difference in the amount of C atom in the elemental analysis results is due to Hb, and based on the data obtained from the N atom, which did not exist before in TASPIONs and 3APGASPIONs and originates from the amine group, which is one of the basic groups of amino acids, Hb binds to the support material. When the results of the cyclic voltogram measurements of TASPIONs and 3APGASPIONs are examined, the Fe(III)/Fe(II) reduction and oxidation reactions of the iron atom in the center of the heme groups of the Hb are seen in the voltograms. Hb took oxygen and gave an oxidation peak at the cathodic potential of −0.418 and −0.398 V, respectively, against the Ag/AgCl standard electrode. It has been reduced to Fe (II) form, which has peaked at −0.145 and −0.136 V anodic potential by giving the oxygen that Hb receives. Accordingly, the difference between the anodic and cathodic battery potentials is 0.273 and 0.262 V, which indicates a fast electron transfer. The formal potential was calculated as −0.2815 and −0.267 V (Pei et al., 2010). The peaks of anodic and cathodic reactions are almost symmetrical and have equal currents. The data may suggest that Hbs are reduced by gaining electrons during negative scanning and completely oxidized by taking back the potential as much as it gives when positive scanning is done (Xu et al., 2013). Repetition studies show that the voltograms overlap and the expected reduction and oxidation reaction proceeds without creating any change in the structure of Hb. When the CV of the suspension containing only the support material is examined; it is seen that no peak is obtained. This shows that the redox reaction does not occur in the support material. When the CV of the solution containing only Hb was analyzed, a peak at −0.468 V cathodic potential and −0.06 V anodic potential was observed against Ag/AgCl standard electrode. The anodic and cathodic potential peaks of TASPIONs-Hb are higher than the peaks obtained from Hb. It may be suggested that the Hb remains almost unchanged and that the number of Hb bound to TASPIONs contains more Hb molecules than the same volume of pure Hb solution after immobilization (Xu et al., 2013).

4.2. The effect of synthesized complexes on endothelial cell functions and antioxidant system

It was detected according to the data that we have obtained that the application of Hb, SPIONs, 3APGASPIONs did not cause a positive proliferative effect on vascular endothelial cells ($p < 0.05$), but a statistically significant increase in TASPIONs. It was reported that SPIONs concentrations applied to cell lines have an effect on cellular proliferation (Gholami et al., 2015). The positive effect of cellular growth in low concentration applications has been mentioned (Gholami et al., 2015). This suggests that it is associated with the concentrations applied. It was determined that Hb administration caused a significant increase in SOD ($p < 0.001$) and glutathione peroxidase ($p < 0.01$) enzyme activity (CAT activity is not significant). Pure SPIONs caused an increase in enzyme activity in their CAT ($p < 0.01$), SOD ($p < 0.05$) and glutathione peroxidase ($p < 0.01$). Application of TASPIONs-Hb complex did not cause a statistically significant change in CAT and SOD enzyme activity; however, it increased the GPX activity significantly ($p < 0.01$). While 3APGASPIONs-Hb administration did not cause a significant change in CAT and SOD enzyme activity of endothelial cell, it decreased GPX activity ($p < 0.05$). It has been reported that Hb application to the cell line increases the concentration of reactive oxygen species (ROS) depending on the concentration supporting this study (Lee et al., 2006). The iron of the heme group in free Hb may react with endogenous hydrogen peroxide in order to produce free radicals that cause oxidative cell damage and to accumulate hydroxyl radicals (Melamed-Frank et al., 2001). It was reported that SPIONs may also cause cellular toxicity by damaging the plasma membrane and causing cellular stress (Arimoto et al., 2005; Amara et al., 2007). Furthermore, it was mentioned that coated SPIONs have a lower effect (Häfeli et al., 2009). It has been mentioned that the cytotoxic effect may change depending on the applied concentration and exposure time (Berry et al., 2003).

Declaration of Competing Interest

The authors declare that they have no known competing financial interests or personal relationships that could have appeared to influence the work reported in this paper.

Acknowledgements

This study was supported by Çukurova University Scientific Research Projects Coordination Unit. Project number: TDK-2014-2686.

References

Abo-Zeid, Y., Ismail, N.S., McLean, G.R., et al., 2020. A molecular docking study repurposes FDA approved iron oxide nanoparticles to treat and control COVID-19 infection. Eur. J. Pharm. Sci. 153, 105465.

Alayash, A.I., 2019. Mechanisms of toxicity and modulation of hemoglobin-based oxygen carriers. Shock (Augusta, Ga.) 52 (1 Suppl), 41.

Al-Hamdany, A., Jihad, T., 2012. Oxidation of some primary and secondary alcohols using pyridinium chlorochromate. Tikrit J. Pure Sci. 17 (4).
Amara, N., Bachoual, R., Desmard, M., et al., 2007. Diesel exhaust particles induce matrix metalloprotease-1 in human lung epithelial cells via a NADP (H) oxidase/NOX4 redox-dependent mechanism. American J. Physiol.-Lung Cell. Mol. Physiol. 293 (1), L170–L181.
Arami, H., Khandhar, A., Liggitt, D., et al., 2015. In vivo delivery, pharmacokinetics, biodistribution and toxicity of iron oxide nanoparticles. Chem. Soc. Rev. 44 (23), 8576–8607.
Arimoto, T., Kadiiska, M.B., Sato, K., et al., 2005. Synergistic production of lung free radicals by diesel exhaust particles and endotoxin. Am. J. Respir. Crit. Care Med. 171 (4), 379–387.
Arnone, A., 1974. Mechanism of action of hemoglobin. Annu. Rev. Med. 25 (1), 123–130.
Berry, C.C., Wells, S., Charles, S., et al., 2003. Dextran and albumin derivatised iron oxide nanoparticles: influence on fibroblasts in vitro. Biomaterials 24 (25), 4551–4557.
Cao, M., Wang, G., He, H., et al., 2021a. Hemoglobin-Based Oxygen Carriers: Potential Applications in Solid Organ Preservation. Front. Pharmacol. 12.
Cao, M., Zhao, Y., He, H., et al., 2021b. New Applications of HBOC-201: A 25 year review of the Literature. Front. Med., 2398
Chang, T.M., 1999. Future prospects for artificial blood. Trends Biotechnol. 17 (2), 61–67.
Chang, T.M.S., 2004. Hemoglobin-based red blood cell substitutes. Artif. Organs 28 (9), 789–794.
Chang, T.M.S., 2006. Evolution of artificial cells using nanobiotechnology of hemoglobin based RBC blood substitute as an example. Artif. Cells, Blood Subst., Biotechnol. 34 (6), 551–566.
Chang, T.M.S., 2010. Blood substitutes in 2010. Taylor & Francis. 38, 295–296.
Chawla, S., Pundir, C.S., 2011. An electrochemical biosensor for fructosyl valine for glycosylated hemoglobin detection based on core–shell magnetic bionanoparticles modified gold electrode. Biosens. Bioelectron. 26 (8), 3438–3443.
Darendeli, B., 2014. Dioksim türevi metal komplekslerin depozisyon işlemlerinde öncül olarak kullanılabilirliklerinin incelenmesi, Fen Bilimleri Enstitüsü.
Gholami, A., Rasoul-amini, S., Ebrahiminezhad, A., et al., 2015. Lipoamino acid coated superparamagnetic iron oxide nanoparticles concentration and time dependently enhanced growth of human hepatocarcinoma cell line (Hep-G2). J. Nanomater.
Goorha, Y., Deb, P., Chatterjee, T., et al., 2003. Artifical blood. Med. J. Armed Forces India 59 (1), 45–50.
Greenburg, A.G., Kim, H.W., 2004. Hemoglobin-based oxygen carriers. Crit. Care 8 (2), 1–4.
Gupta, A.S., 2019. Hemoglobin-based oxygen carriers: current state-of-the-art and novel molecules. Shock (Augusta, Ga.) 52 (1), 70.
Häfeli, U.O., Riffle, J.S., Harris-Shekhawat, L., et al., 2009. Cell uptake and in vitro toxicity of magnetic nanoparticles suitable for drug delivery. Mol. Pharm. 6 (5), 1417–1428.
Herold, S., 1998. Kinetic and spectroscopic characterization of an intermediate peroxynitrite complex in the nitrogen monoxide induced oxidation of oxyhemoglobin. FEBS Lett. 439 (1–2), 85–88.
Intaglietta, M., 1997. Whitaker lecture 1996: Microcirculation, biomedical engineering, and artificial blood. Ann. Biomed. Eng. 25 (4), 593–603.
Jadhav, N.V., Prasad, A.I., Kumar, A., et al., 2013. Synthesis of oleic acid functionalized Fe3O4 magnetic nanoparticles and studying their interaction with tumor cells for potential hyperthermia applications. Colloids Surf. BBiointerfaces. 108, 158–168.
Keyhanian, S., Ebrahimifard, M., Zandi, M., 2014. Investigation on artificial blood or substitute blood replace the natural blood. Iranian J. Pediatric Hematol. Oncol. 4 (2), 72.
Kim, H.W., Greenburg, A.G., 2004. Artificial oxygen carriers as red blood cell substitutes: a selected review and current status. Artif. Organs 28 (9), 813–828.
Kim, J.S., Yoon, T.-J., Yu, K.N., et al., 2006. Toxicity and tissue distribution of magnetic nanoparticles in mice. Toxicol. Sci. 89 (1), 338–347.
Lee, R.-A., Kim, H.-A., Kang, B.-Y., et al., 2006. Hemoglobin induces colon cancer cell proliferation by release of reactive oxygen species. World J. Gastroenterol.: WJG 12 (35), 5644.
Lieberthal, W., Fuhro, R., Andry, C., et al., 2000. Effects of hemoglobin-based oxygen-carrying solutions in anesthetized rats with acute ischemic renal failure. J. Lab. Clin. Med. 135 (1), 73–81.
Liu, C.-H., Sahoo, S.L., Tsao, M.-H., 2014. Acridine orange coated magnetic nanoparticles for nucleus labeling and DNA adsorption. Colloids Surf. BBiointerfaces. 115, 150–156.
Lowe, K., 1999. Perfluorinated blood substitutes and artificial oxygen carriers. Blood Rev. 13 (3), 171–184.
Lu, Y., Yin, Y., Mayers, B.T., et al., 2002. Modifying the surface properties of superparamagnetic iron oxide nanoparticles through a sol– gel approach. Nano Lett. 2 (3), 183–186.
Mahmood, I., Ahmad, I., Chen, G., et al., 2013. A surfactant-coated lipase immobilized in magnetic nanoparticles for multicycle ethyl isovalerate enzymatic production. Biochem. Eng. J. 73, 72–79.
Melamed-Frank, M., Lache, O., Enav, B.I., et al., 2001. Structure-function analysis of the antioxidant properties of haptoglobin. Blood, J. American Soc. Hematol. 98 (13), 3693–3698.
Mohanto, N., Park, Y.-J., Jee, J.-P., 2022. Current perspectives of artificial oxygen carriers as red blood cell substitutes: a review of old to cutting-edge technologies using in vitro and in vivo assessments. J. Pharm. Investig., 1–38
Özdemir, M.D., 2006. Atmalı plazma katodik ark yöntemi ile elde edilen ZnO ince filmlerin optik ve yapısal özellikleri, Fen Bilimleri Enstitüsü.
Pei, S., Qu, S., Zhang, Y., 2010. Direct electrochemistry and electrocatalysis of hemoglobin at mesoporous carbon modified electrode. Sensors 10 (2), 1279–1290.
Polakovs, M., Mironova-Ulmane, N., Pavlenko, A., et al., 2012. EPR and FTIR spectroscopies study of human blood after irradiation. Spectroscopy: Int. J. 27 (5–6), 367–371.
Rezaeifard, A., Jafarpour, M., Naeimi, A., et al., 2012. Aqueous heterogeneous oxygenation of hydrocarbons and sulfides catalyzed by recoverable magnetite nanoparticles coated with copper (II) phthalocyanine. Green Chem. 14 (12), 3386–3394.
Sarkar, S., 2008. Artificial blood. Indian J. Crit. Care Med.: Peer-Reviewed, Official Publication of Indian Society of Critical Care Medicine 12 (3), 140.
Sharma, S., Sharma, P., Tyler, L.N., 2011. Transfusion of blood and blood products: indications and complications. Am. Fam. Physician 83 (6), 719–724.
Shriver, D.F., Atkins, P., Özkar, S., et al., 1999. Anorganik kimya, Bilim Yayıncılık.
Simek, J.W., Tuck, T., Bush, K.C., 1997. Reduction of carboxylic acids with sodium borohydride and an electrophile. J. Chem. Educ. 74 (1), 107.
Smith, A., McCulloh, R.J., 2015. Hemopexin and haptoglobin: allies against heme toxicity from hemoglobin not contenders. Front. Physiol. 6, 187.
Takeoka, S., 2005. Developmental trend of artificial blood (artificial red blood cells). Japan Med. Assoc. J. 48, 135–139.
Tang, T., Fan, H., Ai, S., et al., 2011. Hemoglobin (Hb) immobilized on amino-modified magnetic nanoparticles for the catalytic removal of bisphenol A. Chemosphere 83 (3), 255–264.
TJ, R., 2003. Hb-based oxygen carriers: are we there yet. Transfusion 43, 280–287. 737.
Ün, M., Erbaş, O., 2019. Artificial blood. Demiroğlu Bilim Üniversitesi Florence Nightingale Transplantasyon Dergisi. 4 (1), 041–045.
Xu, M.-Q., Wu, J.-F., Zhao, G.-C., 2013. Direct electrochemistry of hemoglobin at a graphene gold nanoparticle composite film for nitric oxide biosensing. Sensors 13 (6), 7492–7504.
Yaşar, Ü. 2016. The development of support biomaterial that for transporting of oxygen in the blood. Cukurova University, Health Sciences Institute, Department of Medical Biochemistry, PhD thesis, pp: 151., Adana, Türkiye
Yaşar, Ü., Huri, P.Y., Dikmen, N., 2012. Yapay Kan. Arşiv Kaynak Tarama Dergisi 21 (2), 95–108.